Journal of Solid State Chemistry 258 (2018) 768–775

Contents lists available at ScienceDirect

Journal of Solid State Chemistry

journal homepage: www.elsevier.com/locate/jssc

Thermoelectric and magnetic properties of Cr-doped single crystal Bi_2Se_3 – Search for energy filtering

P. Cermak[a], P. Ruleova[a], V. Holy[b,c], J. Prokleska[b], V. Kucek[a], K. Palka[a,d], L. Benes[a], C. Drasar[e,*]

[a] Department of General and Inorganic Chemistry, Faculty of Chemical Technology, University of Pardubice, Studentska 573, 532 10 Pardubice, Czech Republic
[b] Department of Condensed Matter Physics, Faculty of Mathematics and Physics, Charles University, Ke Karlovu 3, 121 16 Praha 2, Czech Republic
[c] Masaryk University, Department of Condensed Matter Physics and CEITEC, Kotlářská 2, 61137 Brno, Czech Republic
[d] Center of Materials and Nanotechnologies - CEMNAT, Faculty of Chemical Technology, University of Pardubice, nam. Cs. legii 565, 530 02 Pardubice, Czech Republic
[e] Institute of Applied Physics and Mathematics, Faculty of Chemical Technology, University of Pardubice, Studentska 573, 532 10 Pardubice, Czech Republic

ARTICLE INFO

Keywords:
Thermoelectrics
Single crystal
Transition metal doping
Energy filtering
Tetradymite

ABSTRACT

Thermoelectric effects are one of the promising ways to utilize waste heat. Novel approaches have appeared in recent decades aiming to enhance thermoelectric conversion. The theory of energy filtering of free carriers by inclusions is among the latest developed methods. Although the basic idea is clear, experimental evidence of this phenomenon is rare. Based on this concept, we searched suitable systems with stable structures showing energy filtering. Here, we report on the anomalous behavior of Cr-doped single-crystal Bi_2Se_3 that indicates energy filtering. The solubility of chromium in Bi_2Se_3 was studied, which is the key parameter in the formation process of inclusions. We present recent results on the effect of Cr-doping on the transport coefficients on a wide set of single crystalline samples. Magnetic measurements were used to corroborate the conclusions drawn from the transport and X-ray measurements.

1. Introduction

Bi_2Se_3, which adopts the tetradymite structure, is one of the constituents of room-temperature thermoelectric (TE) materials [1]. Some of these tetradymite materials have been shown to form diluted magnetic semiconductors (DMS) if they are doped with certain transition metals (TM). A variety of magnetic ordering has been reported, although the interactions leading to the ordering is still subject to discussion [2–6]. The reason is that there are most likely two or more types of interactions in each TM doped sample. The discovery that these materials are 3D topological insulators (TI) [7–9] has led to renewed attention to doping these materials with magnetic impurities. Among many other materials, Bi_2Se_3 is the most promising for electronic applications since its surface states consist of a single Dirac cone, and the material has a reasonably large band gap to guarantee an eventually very low bulk electrical conductivity. The common point to all the works is the spin manipulation. The Ferromagnetism (FM) in Cr-doped [10,11] or Cr-intercalated [12] Bi_2Se_3 has been reported for MBE thin films. Contrarily, an antiferromagnetic (AFM) ordering has been reported for one sample of a Cr-doped Bi_2Se_3 single crystal [13]. All reports differ in properties and solubility for the magnetic impurity, and the authors admit that an interaction leading to a magnetic ordering is still unclear and call for further studies. There are profound theoretical calculations reported on the energy formation of defects [e.g., 14], which are very helpful as a guide in terms of tendencies along the periodic table (e.g., V, Cr, Mn, and Fe). Although Ref. [14] suggests a slightly negative formation energy of Cr point defects in place of Bi, Cr_{Bi}, (i.e., spontaneous formation of such defects), we found the actual concentration of Cr is always lower than the nominal one in our single crystals, which indicates the opposite. Moreover, we found a tendency of clustering when the single crystals are forced to incorporate higher concentrations of Cr during growth from a Cr-rich melt e.g., in Bridgman crystal; Fig. 5 (below) shows an XRF mapping of Cr close to the end (head) of the Bridgman single crystal for x = 0.01. In addition, other phases ($BiCrSe_3$, $Bi_2Cr_4Se_9$) appear for x ≥ 0.02 in the XRD patterns of our single crystals. This is in accordance with the phase diagram indicating the solubility of Cr in the solid Bi_2Se_3 is close to zero, while the liquid state Bi_2Se_3 dissolves up to 20% of Cr_2Se_3 at 1170 K [15]. Two incongruent compounds are formed in the pseudo-binary phase diagram: the daltonide $Bi_2Cr_4Se_9$, and the berthollide with an approximate composition of $BiCrSe_3$ (γ-phase, $Bi_5Cr_4Se_{13}$). An extraordinary

* Corresponding author.
E-mail address: cestmir.drasar@upce.cz (C. Drasar).

https://doi.org/10.1016/j.jssc.2017.12.009
Received 19 October 2017; Received in revised form 6 December 2017; Accepted 7 December 2017
Available online 10 December 2017
0022-4596/

paramagnetism is reported in Bi-Cr-Se ternary misfit-layer compounds based on these two compounds [16].

Following these results, we aim to prepare single-crystal $Bi_{2-x}Cr_xSe_3$ as close to equilibrium as possible for a given temperature to provide a detailed comparison for theoretical and experimental works. The motivation is to provide more insight into the TM-doped tetradymites. There are many uncertainties, including that the equilibrium solubility is lower than that expected from the theoretical predictions. Contrary to some papers [10–13], our results suggest that both AFM and FM ordering exist next to paramagnetism (PM) in this material. Notably, we show that doping with TM might be interesting in terms of TE applications. Namely, TMs are candidates for extra energy filtering of free carriers, which is a way to increase the efficiency of TE materials [17–19]. We think that nano-structuring may explain the extraordinary behavior. We are aware that many questions are not satisfactorily answered, but we hope they can serve as an inspiration.

2. Experiment

Single crystals of $Bi_{2-x}Cr_xSe_3$, with nominal x values between 0 and 0.04, were grown by heating stoichiometric mixtures of 5N Bi, Se and Cr_2Se_3. The synthesis of Cr_2Se_3 was carried out by heating stoichiometric mixtures of 5N purity elements at 1300 K for 7 days in quartz ampoules (all from Sigma-Aldrich). The crystal growth process involved cooling from 1073 K to 823 K at a rate of 6 K per hour. The crystals were then annealed for 500 h at 823 K in the same ampoule and then quenched in air. This free melt crystallization (FMC) produces single crystals that are 10–20 mm in length, 3–6 mm wide and up to 3 mm thick. In addition, $Bi_{2-x}Cr_xSe_3$ single crystals were grown using the Bridgman technique (BT) to better understand the behavior of Cr during growth. Contrary to FMC, the BT shows a directional crystallization par excellence. Thus, the liquidus–solidus distribution coefficient of the dopant in the Bi_2Se_3 plays an important role. Mostly, the solubility of the doping TM is higher in the liquid phase, as is in case of Cr, and the liquid phase becomes richer in Cr along the direction of crystal growth. Thus, the concentration of chromium increases along the single crystals up to the highest solubility, after which precipitates are eventually formed at a given temperature. The BT produces single crystals up to 60 mm in length, 8 mm wide and 5 mm thick. The orientation of all single crystals was determined using the single-crystal X-ray technique. For the physical property measurements, the FMC specimens with dimensions of 10–15 × 3 × (0.1–0.2) mm^3 were cut from the single crystals. The actual doping level and macroscopic homogeneity was examined using XRF mapping with a μ-XRF spectrometer M4 TORNADO (Bruker), Rh-50 keV, equipped with polycapillary X-ray optics. To reveal the microscopic homogeneity, we employed energy dispersive X-ray microanalysis (EDX) using scanning electron microscopy (SEM) LYRA 3 (Tescan) equipped with an EDX analyzer Aztec X-Max 20 (Oxford Instruments).

The diffraction patterns (Cu Kα, λ = 1.5418 Å) were recorded on powdered samples using a D8 Advance diffractometer (Bruker AXES, Germany) with a Bragg–Brentano Θ-Θ goniometer (radius 217.5 mm) equipped with a Ni-beta filter and a LynxEye detector. The scan was performed at room temperature from 10 to 90° (2Θ) in 0.01° steps with a counting time of 2 s per step. The lattice parameters were refined using the Le Bail method as implemented in the program FullProf.

High-resolution X-ray diffraction (HR XRD) on single-crystalline $Bi_{2-x}Cr_xSe_3$ samples was carried out on a PaNalytical Expert-Pro diffractometer, equipped with a sealed CuKα tube, primary parabolic multilayer optics, a 2x220Ge single-crystal monochromator, a 3x220Ge analyzer, and a proportional point detector. Using this high-resolution setup, we were able to measure the reciprocal-space distribution of the diffracted intensity with a resolution down to 10^{-4} $Å^{-1}$.

The transport parameters include the electrical conductivity $\sigma(i\perp c)$, the Hall coefficient $R_H(B||c)$, and the Seebeck coefficient $S(\Delta T\perp c)$. These parameters were measured in the direction perpendicular to the trigonal axis, *c*, i.e., the electric field and thermal gradients were applied in the basal plane while the magnetic induction vector was parallel to the *c* axis. All parameters were measured over a temperature range from 80 K to 470 K, and a conductive graphite adhesive was used to attach the current leads. Platinum wires (50 μm in diameter) were attached along the sample using thermocompression to measure the voltage drop. The Hall effect and electrical conductivity were examined using a lock-in nano-voltmeter with a 29-Hz excitation and a static magnetic field of 0.6 T. The Seebeck coefficient was determined using the longitudinal steady-state technique with a temperature difference ranging from 3 to 3.5 K. The thermal gradients were measured with the aid of fine copper-constantan thermocouples. The magnetic properties were investigated using an MPMS apparatus (Quantum Design).

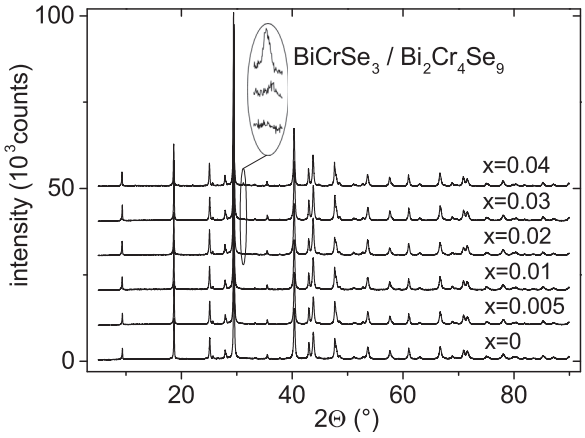

Fig. 1. XRD patterns of $Bi_{2-x}Cr_xSe_3$ single crystals for nominal x = 0–0.04. There is clear evidence of an additional phase (peak at 2Θ = 31.3°) for x = 0.03 and 0.04, which can be attributed to either $BiCrSe_3$ or $Bi_2Cr_4Se_9$. This peak is barely detectable for nominal x = 0.02. The patterns are shifted vertically for clarity.

3. Results and discussion

3.1. X-ray analysis, XRF analysis, SEM

Typical X-ray diffraction patterns of $Bi_{2-x}Cr_xSe_3$ obtained for powdered single crystals are shown in Fig. 1. Although all the diffraction peaks can be attributed to the structure of the Bi_2Se_3 for x ≤ 0.01, there is clear evidence of additional phases (one peak at 2Θ = 31.3° attributable to both the $Bi_2Cr_4Se_9$ and γ-phase (approximate composition $BiCrSe_3$)) at x = 0.03 and x = 0.04. This peak is barely detectable for a nominal composition $Bi_{1.98}Cr_{0.02}Se_3$, even for very fine measurements. Thus, the equilibrium solubility of Cr in Bi_2Se_3 at 820 K lies below x = 0.02. For the TE, this is the nominal concentration over which the micro-precipitates (X-ray detectable) of other phases might form. Thus, the nano-precipitates might form at far lower Cr concentrations depending on the growth kinetics. The lattice parameters of the parent material, *a* = 0.41387 nm and *c* = 2.86303 nm, are in good agreement with those in the database (PDF-4+/ICDD). We observe that the lattice parameters decrease moderately with the increase of the Cr concentration. Table 1 summarizes the lattice parameter values of *a* and *c* for $Bi_{2-x}Cr_xSe_3$. Note that although the actual concentrations of the dopant are small, the crystal radii of the substitutional Cr ($r(Cr^{+3})$ = 0.0755 nm and $r(Cr^{+2})$ = 0.094 nm) are much smaller than that of Bi ($r(Bi^{+3})$ = 0.117 nm) [20]. The slight but measurable drop from doping is close to the experimental errors according to our measurements. Thus, we can observe some solubility of Cr in Bi_2Se_3, but we are not able to discuss the solubility of Cr within Vegard´s law.

Figs. 2–4 show the results of the HR XRD diffraction experiments. In Fig. 2, we plotted the symmetric 2theta/omega scan measured on the Bi_2Se_3 and $Bi_{2-x}Cr_xSe_3$ (x = 0.01) single crystals (points) along with the simulations (lines). Since the sample surface was (0001), the scan